Talanta 251 (2023) 123793

Contents lists available at ScienceDirect

Talanta

journal homepage: www.elsevier.com/locate/talanta

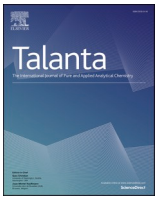

Anchoring red blood cell with tetrahedral DNA nanostructure: Electrochemical biosensor for the sensitive signage of circulating tumor DNA

Xinyue Zha [a], Weiwei Qin [c], Jiadi Chen [a], Mengting Chen [a], Qiyue Zhang [a], Kaiyu He [b,**], Yingju Liu [a,*], Weipeng Liu [a,***]

[a] Key Laboratory for Biobased Materials and Energy of Ministry of Education, College of Materials and Energy, South China Agricultural University, Guangzhou, 510642, China

[b] State Key Laboratory for Managing Biotic and Chemical Threats to the Quality and Safety of Agro-products, Institute of Agro-product Safety and Nutrition, Zhejiang Academy of Agricultural Sciences, Hangzhou, 310021, China

[c] Zhejiang Provincial Key Laboratory of Biometrology and Inspection and Quarantine, College of Life Science, China Jiliang University, Hangzhou, 310018, China

ARTICLE INFO

Keywords:
Tetrahedral DNA nanostructures
Electrochemical biosensor
Circulating tumor cells
ctDNA
Methylene blue

ABSTRACT

Circulating tumor cells (CTCs), as a type of tumor, have attracted wide attention because of their characteristics of shedding from the primary tumor and spreading to other tissues and organs through peripheral blood. The circulating tumor DNA (ctDNA), the DNA released by CTCs and other tumor cells into the peripheral blood, was considered as a promising detection substance for clinical application. By utilizing the biocompatibility of red blood cells to realize the attachment of tetrahedral DNA (TDN), as well as the specific target recognition ability of TDN to enable efficient recognition of targets, a biocompatible electrochemical biosensor for effective and rapid detection of ctDNA was developed using methylene blue (MB) as the signal probe. The current signal and the logarithm of ctDNA concentration were linearly correlated in the range from 1 fM to 100 pM with the detection limit of 0.66 fM. With high specificity, the TDN-based biosensor can detect ctDNA efficiently in the real biological environment such as serum, which provided a potential opportunity for the early clinical diagnosis.

1. Introduction

According to the report of the World Health Organization (WHO), cancer, as one of the most malignant diseases, poses a great threat to human beings. The mortality and incidence of cancer are rapidly rising around the world every year, even causing millions of deaths [1]. 90% of cancer-related deaths are mainly caused by cancer metastasis. Circulating tumor DNA (ctDNA) is the DNA released by necrotic and apoptotic tumor cells or circulating tumor cells into the peripheral blood. Relevant studies have found that many genetic and epigenetic abnormalities related to malignant tumors including heterozygosity deletion, gene amplification and single nucleotide mutation have been detected in ctDNA. Therefore, ctDNA has been used as a potential biomarker to achieve early diagnosis, monitoring and evaluation of tumors in the clinical field [2,3]. However, the size of ctDNA is extremely small and its content in the blood varies according to the severity of the tumor. Especially in the early stage of the tumor, the content may even be lower than 0.1%. In addition, the difference between ctDNA and normal DNA fragments is very small, so ctDNA can be hidden in numerous normal DNA fragments [4]. Due to the rarity and variability of ctDNA, it is essential to establish a highly specific and sensitive approach for ctDNA detection.

Traditional ctDNA detection methods include dPCR (digital polymerase chain reaction), BEAMing (bead, emulsion, amplification and magnetic), ARMS-PCR (amplification refractory mutation system-polymerase chain reaction), etc. The ddPCR (droplet digital PCR) can be used to realize the measurement of the allele frequencies in small fragments from four L858R mutation ctDNA samples [5]. However, some shortcomings of ddPCR, such as the generated droplets must obey the Poisson distribution, and only a limited number of mutations can be

* Corresponding author.
** Corresponding author.
*** Corresponding author.
E-mail addresses: hekaiyu@zaas.ac.cn (K. He), liuyingju@hotmail.com, yingjuliu@scau.edu.cn (Y. Liu), weipeng_liu@scau.edu.cn (W. Liu).

https://doi.org/10.1016/j.talanta.2022.123793
Received 14 May 2022; Received in revised form 21 July 2022; Accepted 26 July 2022
Available online 5 August 2022

detected per assay, can be comprehensively discovered. The BEAMing technology can be used to achieve the identification of mutated genes by measuring the ctDNA and mutKRAS among 284 plasma samples from the advanced PC patients [6]. Although the BEAMing can be used to identify, screen and isolate rare mutation-specific ctDNA, it can be only applied to detect known mutations, while the disadvantages such as high cost and complicated operation should be considered. AS-PCR (Allele-specific PCR), also known as ARMS-PCR (Mutation Amplification Blockade System PCR), can be used to detect two or more allele mutation sites in the same system simultaneously [7]. However, the false positive rate is relatively high, while the reaction conditions in the early stage should be intensively optimized.

Recently, the electrochemical detection has been widely developed for diagnosing ctDNA [8]. Compared with the above ctDNA detection methods, the electrochemical detection is simple, sensitive, timeliness and cheap [9,10]. The electrochemical biosensor for DNA detection was realized by converting the amount of DNA to electrochemical signal. For an instance, the polyacrylamide/phytic acid/dopamine hydrogels were modified on glassy carbon electrode (GCE) to achieve adsorption and desorption of single-stranded DNA (ssDNA) by electric field driving, thus a rapid and efficient recognition of ssDNA has been fabricated for the electrochemical detection of ctDNA [11]. Gold nanoparticles (Au NPs) were modified on GCE to capture the DNA probe through Au–S bond, thus the ctDNA can be detected by using the methylene blue (MB) as electroactive indicator [12]. Aiming at increasing the amount of signal probe, a novel approach to detect ctDNA was designed by introducing tetrahedral DNA nanostructure (TDN) as a signal marker. Comparing with other nanoparticles used in biosensors, TDN can be synthesized by four ssDNA through simple one-step self-assembly, which was simpler and more controllable [13–15]. Therefore, TDN could be widely used in biosensors from heterogeneous surfaces to uniform solutions and from intracellular to extracellular settings for the sensitive detection of targets. In addition, comparing with ssDNA, TDN had higher rigid structure, anti-degradation stability and biocompatibility, which could reduce the possibility of interference and make the results more credible [16,17]. Thus, due to simple synthesis, controllable size, high yield, low cytotoxicity, good biocompatibility and stable structure, TDN has been found comprehensive application in the biosensors, drug delivery, biological imaging and medical separation and analysis [18,19].

Except for the signal probe, the capture probe that can specifically recognize the target sequence is also significant. The common method of detecting ctDNA by fusing TDN and electrochemical sensing, such as immobilizing TDN on the electrode surface, realized the detection of the target. Most of these methods required complex incubation and modification process, as well as the introduction of enzymes or other signal molecules, which were undoubtedly complicate. At the same time, most electrochemical biosensors introduced foreign substances to detect ctDNA in blood, which may cause damage to substances in blood (such as cells), resulting in deviations between the experimental and the actual results. Therefore, the red blood cells were introduced. As we know that the red blood cells widely existed in whole blood, their low cytotoxicity and biocompatibility can make red blood cells as suitable candidate for the part of an electrochemical biosensor [20,21], which can detect ctDNA in blood without introducing foreign substances, and reduce the occurrence of false positive results. Therefore, the combination of red blood cells with TDN in electrochemical biosensors is suitable for detecting ctDNA in blood.

Herein, a biocompatible electrochemical biosensor based on tetrahedral DNA nanostructure was developed to detect ctDNA, providing a new and effective way to detect the DNA of circulating tumor cells. By using red blood cells with low cytotoxicity and biocompatibility to capture ctDNA, and shape-controllable and stable TDN to recognize ctDNA, the target ctDNA could be sandwich recognized by complementary base pairing between DNA strands. After adding MB to the supernatant of TDN, the interaction between MB and TDN can cause different electrochemical signals to reflect the concentrations of ctDNA. The construction of the TDN-based biosensor may greatly expand the application field of early clinical diagnosis and analysis of cancer cell genetic material.

2. Experimental section

2.1. Reagents and apparatus

All DNA sequences, as shown in Table S1, were from Shanghai Sangon Biotechnology (Shanghai, China). Tris-ethylenediaminetetraacetic acid buffer (TE, pH 8.0) and phosphate buffered saline (PBS, pH 7.4) were also bought from Shanghai Sangon Biotechnology (Shanghai, China). MB was from Guangzhou Chemical Reagent Factory (Guangzhou, China). Trimethylolaminomethane hydrochloride (Tris-HCl) was obtained from McLean Biochemical Technology Co., Ltd. (Shanghai, China). Indium tin oxide (ITO) glass was from Shenzhen Nanbo Display Technology Co., Ltd. (Shenzhen, China).

2.2. Apparatus and instrumentation

Agarose gel electrophoresis and atomic force microscope (AFM, Santa Barbara) were applied to investigate the formation of TDN. Agarose gel (2%) electrophoresis analysis was performed in TBE buffer (0.2 mM EDTA, 9 mM boric acid, 9 mM Tris-HCl, pH 7.9) at 110 V for 1 h. For the electrochemical analysis, the differential pulse voltammogram (DPV) measurements were performed with an electrochemical workstation (Chenhua, Shanghai). A standard three-electrode system was employed including an ITO working electrode with an area of 0.125 cm^2 (0.5 cm × 0.25 cm), a platinum wire counter electrode, and an Ag/AgCl reference electrode. After sonicating in ethanol and ultrapure water for 30 min, respectively, the ITO electrode was immersed into 1 mM NaOH for 5 h and sonicated in ultrapure water for another 10 min.

2.3. Preparation of tetrahedral DNA nanostructures

The four strands (100 μM) of ss-A, ss-B, ss-C and ss-D were diluted to 1 μM respectively, and then quantified by UV spectroscopy. The concentration of DNA strand was calculated according to the absorption at about 260 nm and 340 nm based on the following Beer-Lambert Law:

$$C = [(A_{260nm} - A_{340nm})/\text{Extinction coefficient}] \times \text{Dilution multiple} \quad (1)$$

where A_{260nm} and A_{340nm} refereed to the adsorption intensity of DNA strand at 260 nm and 340 nm, respectively. The TM buffer solution (50 mM $MgCl_2$, 20 mM Tris, pH 8.0) was used as the solvent. By mixing the concentration of the four chains at the ratio of 1:1:1:1, a high-temperature denaturation at 95 °C for 10 min and a further low-temperature annealing at 4 °C for 10 min were employed. Thus, the TDN was synthesized and the final concentration was tested as 2.63 μM.

2.4. Pretreatment of red blood cells

The blood taken from the mice was washed several times as follows: 20 μL blood was added to each centrifuge tube containing 1 mL PBS buffer, and then centrifuged twice at 10 °C, 300 rcf and 3 min to remove the supernatant. The washed red blood cells were collected for subsequent use.

After that, the above red blood cells were treated by incubating with the cholesterol-modified DNA1 strands as follows: 9 μL red blood cells, 27 μL PBS and 9 μL cholesterol-modified DNA1 chain (100 μM) were mixed in a centrifuge tube and incubated for 30 min. Then 1 mL PBS was added and then centrifuged three times at 10 °C, 300 rcf and 3 min to remove the supernatant. The DNA1-modified red blood cells were collected for subsequent use.

2.5. Construction of TDN-based biosensor for detecting ctDNA

Firstly, 40 μL TDN (2.63 μM) and 10 μL DNA1-modified red blood cells were added to 1 mL diluted ctDNA and incubated for 1 h. After centrifugating at 10 °C, 300 rcf and 5 min, 1 mL of supernatant was taken out for subsequent use. Then, 52.5 μL of 200 μM MB (dissolved and diluted by Tris-HCl) was added into the above supernatant, mixed evenly and incubated for 30 min. By using the working electrode (the pretreated ITO), the counter electrode (Pt) and the reference electrode (Ag/AgCl) for the electrochemical test, the DPV mode was scanned from −0.4 V to 0.0 V.

3. Results and discussion

3.1. Mechanism of TDN-based biosensor for detecting ctDNA

An electrochemical biosensor based on TDN nanostructure with recognition ability was designed for sensitive and selective detection of ctDNA through complementary base pairing between DNA strands. First, as in Scheme 1A, TDN was synthesized by treating four different items of ssDNA (ss-A, ss-B, ss-C, and ss-D) with high-temperature denaturation and low-temperature annealing procedures. At the same time, a long chain combining ssDNA and DNA2 with recognition sites was designed. Consequently, the functionalization of TDN can be realized through the combination of different numbers of long chains. In addition, by accurately controlling the number of DNA2 on TDN, TDN with four different valence states were prepared, so as to investigate the influence of number of DNA2 on the performance.

Second, as in Scheme 1B, red blood cells were modified with the cholesterol-modified DNA1. Since cholesterol could be tightly embedded in the phospholipid bilayer of animal cell membrane [22,23], it was easy to immobilize the cholesterol-modified DNA1 chain on the surface of red blood cell membrane. When the target ctDNA appeared, the 5′-end of ctDNA could be connected with DNA1-modified red blood cells, while the 3′-end of ctDNA could be connected with functionalized TDN (TDN(I) as an example), according to the principle of complementary base pairing. After centrifugation, the red blood cells-DNA1/ctDNA/TDN could be precipitated. Simultaneously, the unreacted TDN(I) in the supernatant could react with MB since MB could be intercalated into the stacked base pairs of DNA [24]. The more the unreacted TDN(I), the fewer free MB in the solution.

Finally, the free MB in the solution could be detected by the ITO electrode. The pretreated ITO electrode was negatively charged, so the positively charged MB can be diffused to the ITO surface, causing a current change. When there was little or no target ctDNA, the amount of TDN(I) in the supernatant was higher, thus more MB can be interclated into TDN(I) and little MB can be detected on ITO. Therefore, by designing such a TDN-based electrochemical biosensor, a novel and efficient method for the detection of ctDNA was provided.

3.2. Characterization of TDN

TDN was synthesized from four different items of ssDNA (ss-A, ss-B, ss-C, and ss-D) through a procedure of high temperature denaturation and low temperature annealing. At the same time, the long chain was designed which can combine the ssDNA with the DNA2 strand with recognition function. In Fig. 1A, the AFM image of TDN showed that TDN could be dispersed in solution without aggregation. From the enlarged view of single TDN (the inset), it could be seen that its three-dimensional structure was about tetrahedron [25]. The unilateral side lengths of TDN were about 13–14 nm (as shown in Fig. 1B), which was consistent with previous reports [26].

Since TDN has four vertexes and every vertex could carry an DNA2, four TDNs with different numbers of DNA2, defined as TDN(I), TDN(II),

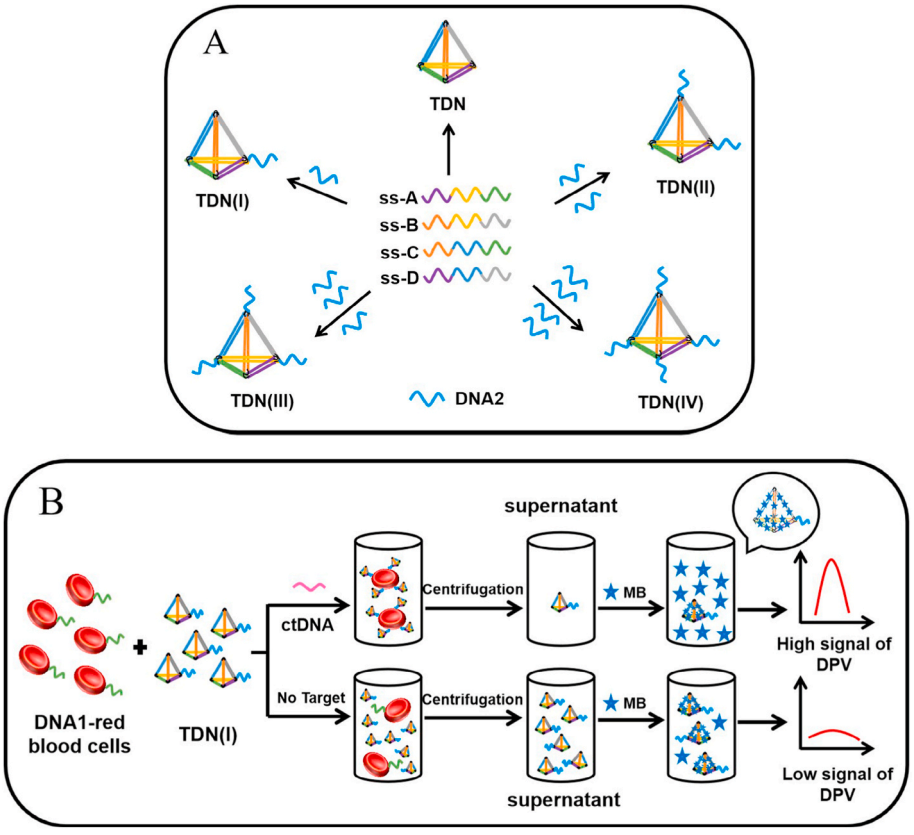

Scheme 1. (A) Synthesis of TDN nanostructures (I, II, III, IV) with 1–4 side chains of DNA2, (B) Principle of electrochemical biosensor for detecting ctDNA based on TDN-anchored red blood cell.

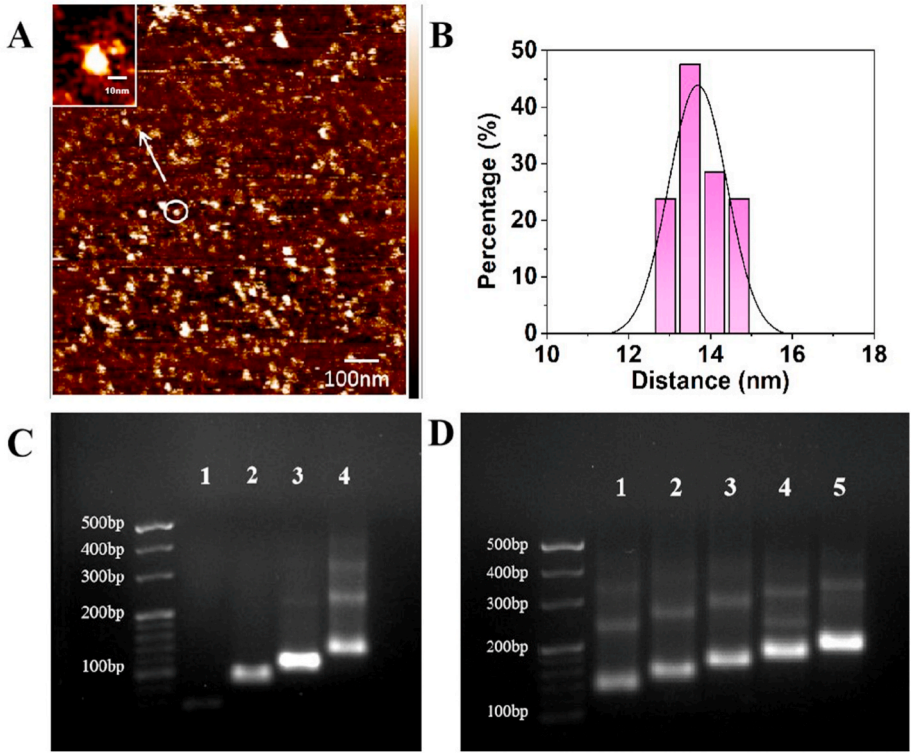

Fig. 1. (A) AFM image of TDN, (B) Particle size distribution of TDN, Agarose gel electrophoresis of different DNA structures, (C) Lane 1: ss-A; Lane 2: a mixture of ss-A and ss-B; Lane 3: a mixture of ss-A, ss-B and ss-D; Lane 4: TDN; (D) Lane 1: TDN; Lane 2: TDN(I); Lane 3: TDN(II); Lane 4: TDN(III); Lane 5: TDN(IV).

TDN(III), and TDN(IV), were prepared by precisely adjusting the number of DNA2 on TDN. In Fig. 1C, the agarose gel electrophoresis showed that the addition of strands from ss-A to ss-D resulted in a gradually decrease in electrophoretic mobility, which was consistent with previous reports [27]. Since the agarose gel electrophoresis was based on the charge effect and molecular sieve effect of DNA molecules in electrophoretic separation, in which molecular sieve effect affects the migration rate of DNA molecules through the size and structure of molecules. As shown in Lane 2, when ss-B was added to ss-A, some bases of ss-A and ss-B were paired to form different structures, which increased the overall relative molecular weight and reduced the mobility of the band. In Lane 3, when ss-D was added, the mixing of three single chains would make more bases complement each other and form a structure with larger molecular weight. Especially, in Lane 4, when four single chains were mixed and incubated, a tetrahedral structure with larger molecular weight was formed, which greatly reduced the migration rate of molecules, implying the TDN was successfully assembled.

Apparently, in Fig. 1D, when the number of DNA2 increased, the motility of the TDN with different valence states decreased significantly. As more DNA2 were carried by TDN, its relative molecular weight increased and the mobility of the band decreased gradually, indicating the successful synthesis of TDN, TDN(I), TDN(II), TDN(III) and TDN(IV) [28]. Hence, the successful self-assembly of the TDN nanostructures was strongly verified. In addition, the stability of TDNs in different solutions (Fig. S1) were investigated. From 0 h to 24 h, the structure of TDNs did not change either in Tris-HCl solution or in PBS solution, indicating the TDNs were stable in both solutions.

3.3. Characterization of red blood cells-DNA1/ctDNA/TDN binding

Circular dichroism spectrometer (CD) was applied to study the connection between DNA strand and red blood cell. CD was the most widely used method for the determination of secondary structure, so the conformation could be preliminarily judged through the different peak positions. According to previous reports [29], the bases of DNA had no intrinsic CD signal, since they were planar. Under the influence of the chiral sugar backbone, the CD signal of the base absorption band can be attributed to the spatial organization of the bases in a chiral structure, such as a helix. Firstly, in Fig. 2A, a positive peak at 275 nm and a negative peak at 245 nm of the ss-A, ss-B, ss-C and ss-D in the CD diagram were discovered, which were characteristic of DNA in right-handed B form in the ultraviolet region [30]. A positive peak at 278 nm and a negative peak at 245 nm of the ctDNA were also discovered in the CD diagram. When the TDN or the TDN(I) was formed, the position of the positive peak didn't change, while a red shift from 245 nm to 248 nm of the negative peak could be found, suggesting that the structure of DNA formed a secondary structure with strong bonding ability from ssDNA [31]. Secondly, in Fig. 2B, negative peaks at 209 nm and 230 nm were discovered for the individual red blood cells. Since the surface of red blood cells were rich in glycoproteins, when the DNA1 strand was inserted into the surface of the cell membrane, the conformation of the cell membrane surface could be changed, causing a blue shift from 230 nm to 222 nm [32,33]. Correspondingly, it could be proved that the DNA1 chain was successfully connected with red blood cells due to the association of cholesterol on the DNA1 chain with the phospholipid bilayer of the cell membrane. Similarly, when the DNA1-modified red blood cells were connected with ctDNA, the peak moved from 222 nm to 228 nm, which was a certain red shift. ctDNA was partially complemented and connected with DNA1, which induced the ssDNA on the surface of cell membrane to form a helical double stranded DNA structure. Then, when the TDN(I) was connected with red blood cell and ctDNA, the peak position moved from 228 nm to 224 nm, which was conversely a little blue shift. The bases did not stack effectively due to the increased distance between the nucleoside bases of TDN(I), which resulted in the shift of the peak position to the short-wave direction. Thus, it was preliminarily proved that the DNA1-modified red blood cells could be combined with ctDNA and TDN(I) as a whole.

After that, laser confocal microscopy was used to further study whether the cholesterol-modified DNA1 chain was successfully connected to red blood cell and whether TDN was connected with red blood

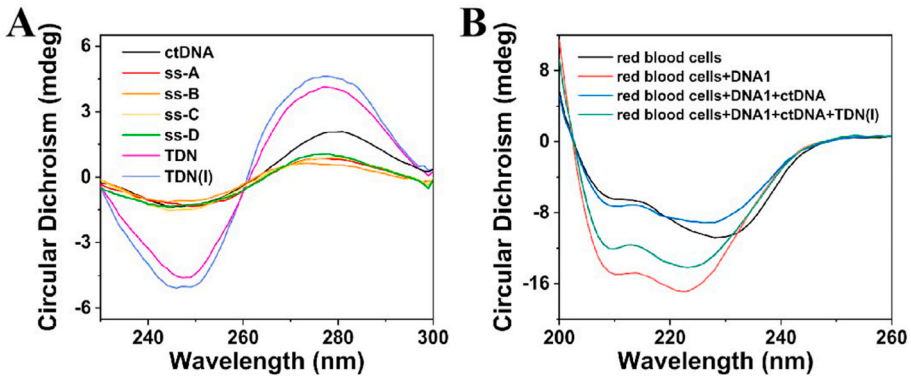

Fig. 2. (A) CD of individual DNA strands, ctDNA, TDN and TDN(I), (B) CD of individual red blood cells and their connection with different DNA strands. (For interpretation of the references to colour in this figure legend, the reader is referred to the Web version of this article.)

cell and ctDNA as a whole. First, the 3′-end of the cholesterol-modified DNA1 chain was decorated with the fluorescent group Cy3 (E_x = 546 nm, E_m = 570 nm, red), while the 3′-ends of ss-A, ss-B and ss-D chains were decorated with the fluorescent group FAM (E_x = 485 nm, E_m = 528 nm, green). Second, ss-C-DNA2 strand (supporting information) and ss-A, ss-B, ss-D modified with fluorophore FAM were used to synthesize TDN(I). Third, the red blood cells were mixed with the fluorophore Cy3-modified DNA1 and incubated for 30 min, followed by incubating with a mixture of ctDNA and TDN(I). Finally, the cells in the bright field were observed (Fig. 3A). In Fig. 3B, obvious red fluorescence was observed around the cells at E_x = 552 nm, which proved the successful connection between the red blood cells and Cy3-DNA1 chain. In Fig. 3C, at E_x = 488 nm, obvious green fluorescence was observed around the cells. Since the cells photographed in different fields were selected from the same position, it could be clearly concluded that the Cy3-DNA1 strand and FAM-TDN(I) were successfully modified at the same position. Fig. 3D was the overlap mapping of bright field and two fluorescence fields. Consequently, according to the spectra of CD spectroscopy and confocal laser microscopy, the modification of DNA on the surface of red blood cells could be successfully carried out. In addition, it was proved that the cholesterol-modified DNA1 chain could be successfully connected to the surface of red blood cells, while TDN(I) could be connected to red blood cells to form a whole composite, in the presence of ctDNA.

3.4. Performance of TDN-based biosensor for detecting ctDNA

First, the DNA ligation ability of MB was verified by using the DPV signal. As shown in Fig. 4, a very strong DPV signal (curve a) could be

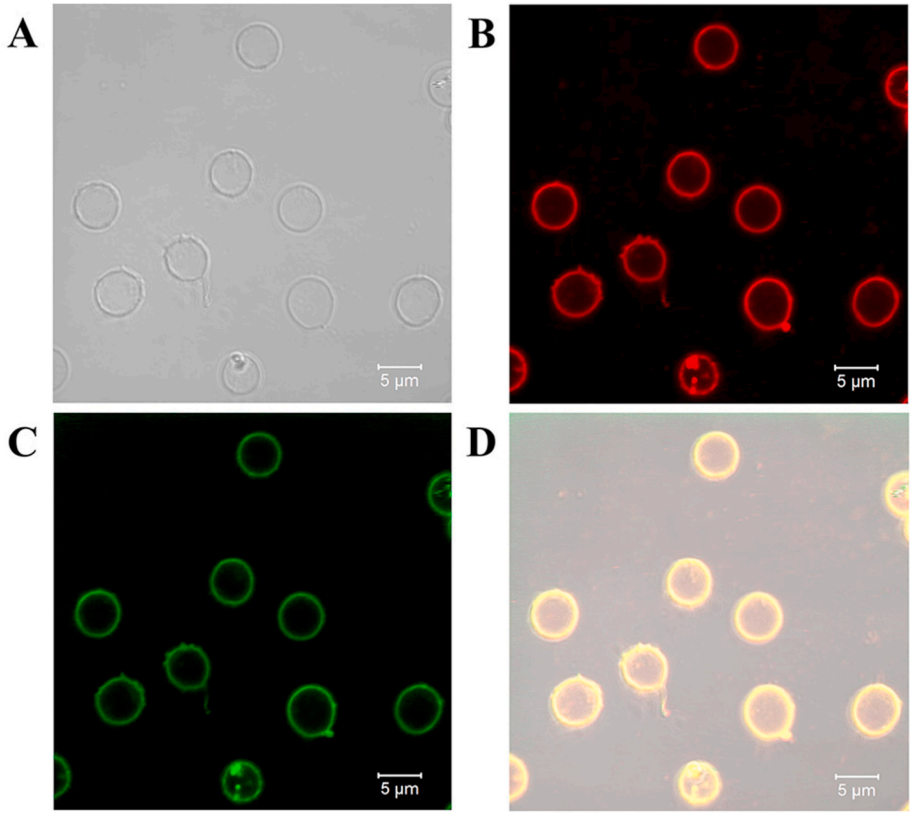

Fig. 3. (A) Laser confocal microscopy images of red blood cells-DNA1/ctDNA/TDN(I) in bright field diagram, (B) in fluorescence field at E_x = 552 nm, (C) in fluorescence field at E_x = 488 nm, and (D) overlay mapping. (For interpretation of the references to colour in this figure legend, the reader is referred to the Web version of this article.)

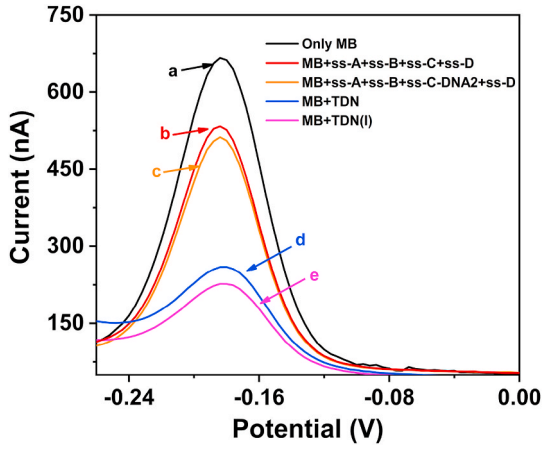

Fig. 4. DPV signals of (a) MB, (b) a simple mixture of MB, ss-A, ss-B, ss-C and ss-D, (c) a simple mixture of MB, ss-A, ss-B, ss-C-DNA2 and ss-D, (d) a mixture of MB and TDN, (e) a mixture of MB and TDN(I).

discovered in 10 μM MB solution (pH 7.4, Tris-HCl solution). After a certain amount of a mixture containing ss-A, ss-B, ss-C and ss-D were added, the DPV signal was significantly reduced (curve b), which mainly contributed to the decrease of electrical signal by electrostatic adsorption between MB and ssDNA [34]. When a certain amount of ss-A, ss-B, ss-C-DNA2 and ss-D were added, the DPV signal (curve c) decreased slightly due to the additional DNA2 segment. However, when a certain amount of TDN was added, the DPV signal decreased more significantly (curve d). MB could be intercalated into the stacked base pairs of dsDNA [35], thus TDN could bind with a larger amount of MB, while a lower amount of the unreacted MB can be detected by negatively charged ITO electrode, resulting in a significant decrease in the DPV signal. Similarly, when a certain amount of TDN(I) was added, the DPV signal decreased slightly (curve e). Thus, comparing with ssDNA, MB could be better inserted into TDN(I), which could significantly change the electrochemical signal of MB.

Next, the experimental conditions for the detection of ctDNA including the MB concentration, the valence numbers of DNA2 to the TDN, the co-incubation time of ctDNA with red blood cells and TDN, and the cholesterol-modified DNA1 chain concentration were optimized. First, Fig. S2 showed the effect of different concentrations of MB on the DPV signal. When the concentration of MB was 10 μM, a higher DPV peak change ($\Delta i_p = i_p\text{-}i_{p0}$, i_{p0} and i_p refer to the DPV signals in the absence and presence of ctDNA) was obtained, so the optimal MB concentration for experiment was 10 μM. Second, the effect of different TDN on the DPV signal was investigated. Four different TDNs were designed to detect the DPV signal of ctDNA at the same concentration. In Fig. S3, a higher DPV signal can be discovered when only one DNA2 was attached to TDN, while the DPV signals of TDN(II), TDN(III) or TDN(IV) were a little lower. First, with the same concentration of DNA1 chain on the surface of red blood cells, they could be connected with more TDN(I), comparing with TDN(II), TDN(III) and TDN(IV). Secondly, since only one strand of TDN(I) was connected to ctDNA and red blood cells, the possibility of spatial effect masking the recognition sites on the surface of red blood cells was reduced. Thus, TDN(I) was selected for the detection of ctDNA. In Fig. S4, when the co-incubation time of ctDNA with red blood cells and TDN was 60 min, a better DPV signal was obtained, so the optimal incubation time was selected as 60 min. Finally, in Fig. S5, at 20 μM of cholesterol-modified DNA1 chain, a best DPV signal was obtained. When the concentration of cholesterol-modified DNA1 chain was too low, red blood cells couldn't bind enough TDN(I); when the concentration of cholesterol-modified DNA1 chains was too high, the binding sites on the surface of red blood cells reached a saturation, thus the optimal concentration of cholesterol-modified DNA1 chain was 20 μM.

Under optimal experimental conditions, the performance of the TDN-based biosensor for ctDNA detection was investigated. When the concentration of the target ctDNA gradually increased, the concentration of TDN in the supernatant decreased, so the free MB in the solution increased, which resulted in a gradual increase in the DPV signal. In Fig. 5A, when the ctDNA concentration increased, the DPV signal of the TDN-based biosensor was gradually enhanced. When the ctDNA concentration range was from 1 fM to 100 pM, the DPV signal and the logarithm of ctDNA concentration were linearly correlated as $I = 13.68 + 75.68c$ ($R^2 = 0.981$), where I was the DPV signal and c was the logarithm of the ctDNA concentration. The limit of detection (LOD) was estimated as 0.66 fM (S/N = 3) (Fig. 5B). Compared with ssDNA and dsDNA, MB could be more effectively inserted into the base pairs of TDN due to its unique structure, forming effective signal amplification. Thus, the analytical performance of the electrochemical biosensor can be compared to or better than the previous work (Table S3).

3.5. Specificity, reproducibility and application in real sample detection

In order to study the specificity of TDN-based biosensors, seven different mutant genes were selected as the experimental group. The RAS gene is the most common oncogene in human tumors. The genes related to human tumors in the RAS gene family are mainly composed of KRAS, NRAS and HRAS. According to the clinical investigation of the relationship between gene mutations and pathological characteristics, the KRAS gene mutation rate is about 32.1%, the PIK3CA gene mutation rate is about 11.3%, the BRAF gene mutation rate is about 6.8%, and the NRAS gene mutation rate is about 5.7% [36]. Therefore, seven nucleotide sequences were selected, including wild-type KRAS gene (wild KRAS), mutant KRAS genes (134C and 135A) and other mutant genes (BRAF, NRAS, EGFR, PIK3CA). In Fig. 5C, the DPV signals of the wild-type gene and the single-base mutant gene significantly decreased compared with the control group, while the current signals of other mutant genes were much weaker, proving that the TDN-based biosensor was suitable for the ctDNA detection. Meanwhile, laser confocal microscope was further used to verify the connection effect of single-base mismatch chain (wild KRAS) and nonspecific chain (BRAF) on red blood cells and TDN(I) (Fig. 6). From Fig. 6B and F, it was clearly observed that Cy3-DNA1 was able to associate with the red blood cell successfully. In Fig. 6C, since there was only one base difference between the wild-type KRAS gene and the target ctDNA, the wild KRAS chain could still be partially connected with red blood cells and TDN(I), and very faint green fluorescence could be discovered. However, in Fig. 6G, the bright green fluorescence could not be discovered, implying that the BRAF mutant gene could not be effectively connected to red blood cells and TDN(I). Comparing the overlay mapping in Fig. 6D and H with Fig. 3D, the electrochemical detection could be further verified. Therefore, the TDN-based biosensor exhibited a certain specificity for the detection of ctDNA.

The reproducibility was analyzed by investigating different experimental groups under the same conditions. As shown in Fig. S6, five groups of independent biosensors were used to detect the same concentration of ctDNA. The differences between different experimental groups were basically negligible, which implied that the TDN-based biosensor showed good reproducibility in the detection of ctDNA.

After that, the TDN-based biosensor was expected to realize the detection of ctDNA in complex biological environment. Different concentrations of ctDNA were added to the diluted serum samples. Table S2 showed that the results of the detection in the serum were the same with those in Tris-HCl, while the recovery rates were ranged from 98.9 to 99.4%, which was attributed to the good biocompatibility and strong anti-enzymatic hydrolysis ability of TDN structure, resulting in less interference of the real environment during the detection process, making the detection results more reliable. Therefore, the TDN-based biosensing method had a great potential for the detection of ctDNA in actual samples.

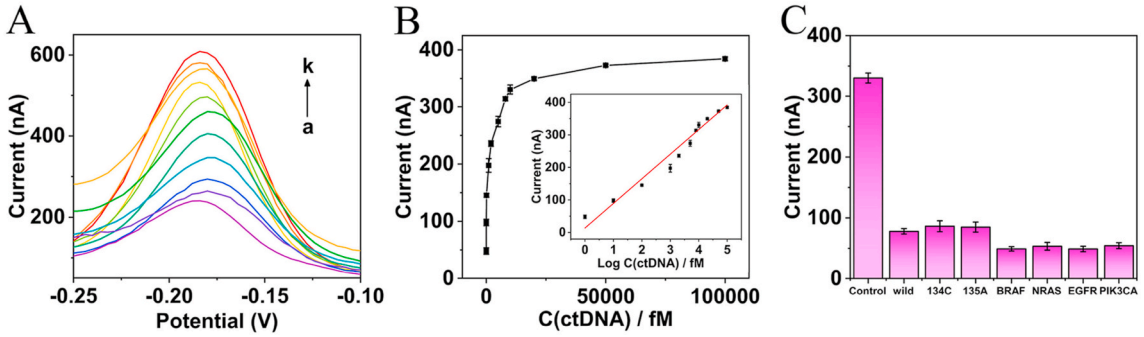

Fig. 5. (A) DPV detection profiles of ctDNA at different concentrations, (a–k)1 fM, 10 fM, 100 fM, 1 pM, 2 pM, 5 pM, 8 pM, 10 pM, 20 pM, 50 pM, 100 pM. (B) The diagram of DPV currents with ctDNA concentrations (Inset: Plot of linear relationship between DPV currents with logarithm of ctDNA concentrations). (C) Specific detection of the TDN-based biosensors (The concentration of each detected DNA strand was 10 pM.).

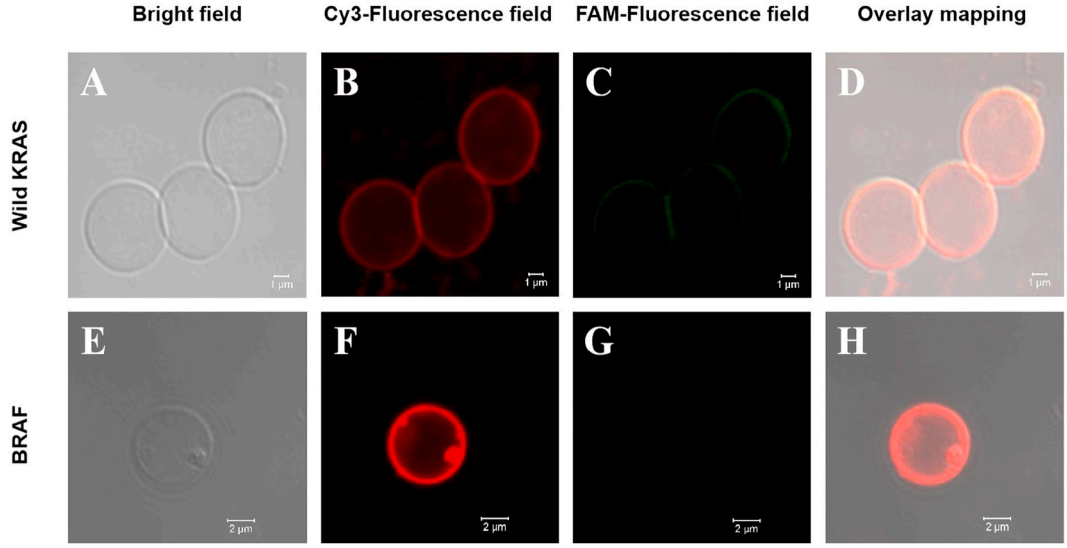

Fig. 6. Laser confocal microscopy images of two different DNA strands including single-base mismatch chain (wild KRAS) and nonspecific chain (BRAF) in bright field (A and E), in fluorescence field at E_x = 552 nm (B and F), in fluorescence field at E_x = 488 nm (C and G), and overlay mapping (D and H).

4. Conclusion

In conclusion, by utilizing the stability and biocompatibility of red blood cells, as well as the high loading rate and specific target recognition ability of TDN, a biocompatible electrochemical biosensor for effective and rapid detection of ctDNA was developed. Since red blood cells exist in large quantities in blood, it was not only more suitable for detection in biological environments such as blood, but also it was not easy to be interfered by other substances in the blood. At the same time, the TDN structure with controllable structure, high load efficiency and specific targeting recognition ability was introduced, which not only avoided the defects of the long-time modification process required by the traditional signal probe, but also could amplify the output of the signal. Benefiting from the effectiveness and convenience, the novel TDN-based biosensing platform realized the detection of ctDNA with high specificity, which exhibited significant analytical application value for clinical diagnosis of target gene.

CRediT author statement

Xinyue Zha: Methodology, Investigation, Formal analysis, Writing – original draft. **Weiwei Qin:** Methodology, Investigation. **Jiadi Chen:** Investigation, Formal analysis. **Mengting Chen:** Investigation. **Qiyue Zhang:** Investigation. **Kaiyu He:** Investigation, Methodology. **Yingju Liu:** Conceptualization, Writing – review & editing, Supervision, Funding acquisition. **Weipeng Liu:** Conceptualization, Writing – review & editing, Supervision, Funding acquisition.

Declaration of competing interest

The authors declare that they have no known competing financial interests or personal relationships that could have appeared to influence the work reported in this paper.

Data availability

Data will be made available on request.

Acknowledgement

This work was supported by the National Natural Science Foundation of China (32170100, 21874048), Science and Technology Program of Guangzhou (202102020511), the Educational Commission Foundation of Guangdong Province (2020ZDZX2025), and Natural Science Foundation of Guangdong Province (2021A1515010208).

Appendix A. Supplementary data

Supplementary data to this article can be found online at https://doi.org/10.1016/j.talanta.2022.123793.

References

[1] F. Bray, J. Ferlay, I. Soerjomataram, R.L. Siegel, L.A. Torre, A. Jemal, Global cancer statistics 2018: GLOBOCAN estimates of incidence and mortality worldwide for 36 cancers in 185 countries, Ca-Cancer. J. Clin. 68 (2018) 394–424.

[2] B. Kwak, J. Lee, J. Lee, H.S. Kim, S. Kang, Y. Lee, Spiral shape microfluidic channel for selective isolating of heterogenic circulating tumor cells, Biosens. Bioelectron. 101 (2018) 311–316.

[3] Y. Wang, Z. Song, X. Hu, H. Wang, Circulating tumor DNA analysis for tumor diagnosis, Talanta 228 (2021), 122220.

[4] T. Hou, N. Xu, W. Wang, L. Ge, F. Li, Truly immobilization-free diffusivity-mediated photoelectrochemical biosensing strategy for facile and highly sensitive microRNA assay, Anal. Chem. 90 (2018) 9591–9597.

[5] N. Yang, Y. Li, Z. Liu, H. Qin, D. Du, X. Cao, X. Cao, J. Li, D. Li, B. Jiang, L. Duan, H. Yang, Z. Zhang, H. Lin, J. Li, Z. Yang, L. Xiong, H. Shen, L. Lin, F. Li, The characteristics of ctDNA reveal the high complexity in matching the corresponding tumor tissues, BMC Cancer 18 (2018) 319.

[6] S. Kruger, V. Heinemann, C. Ross, F. Diehl, D. Nagel, S. Ormanns, S. Liebmann, I. Prinz-Bravin, C.B. Westphalen, M. Haas, A. Jung, T. Kirchner, M.von. Bergwelt-Baildon, S. Boeck, S. Holdenrieder, Repeated (mut)KRAS ctDNA measurements represent a novel and promising tool for early response prediction and therapy monitoring in advanced pancreatic cancer, Ann. Oncol. 29 (2018) 2348–2355.

[7] C.R. Newton, A. Graham, L.E. Heptinstall, S.J. Powell, C. Summers, N. Kalsheker, J. C. Smith, A.F. Markham, Analysis of any point mutation in DNA-the amplification refractory mutation system (ARMS), Nucleic Acids Res. 17 (1989) 2503–2516.

[8] N. Liu, H. Lu, L. Liu, W. Ni, Q. Yao, G. Zhang, F. Yang, Ultrasensitive exosomal microRNA detection with a supercharged DNA framework nanolabel, Anal. Chem. 93 (2021) 5917–5923.

[9] C. Li, D. Wu, X. Hu, Y. Xiang, Y. Shu, G. Li, One-step modification of electrode surface for ultrasensitive and highly selective detection of nucleic acids with practical applications, Anal. Chem. 88 (2016) 7583–7590.

[10] Y. Peng, Y. Pan, Z. Sun, J. Li, Y. Yi, J. Yang, G. Li, An electrochemical biosensor for sensitive analysis of the SARS-CoV-2 RNA, Biosens. Bioelectron. 186 (2021), 113309.

[11] J. Wei, Z. Zhao, J. Gao, Y. Wang, L. Ma, X. Meng, Z. Wang, Polyacrylamide/phytic acid/polydopamine hydrogel as an efficient substrate for electrochemical enrichment of circulating cell-free DNA from blood plasma, ACS Omega 5 (2020) 5365–5371.

[12] M. Mazloum-Ardakani, M.M. Heidari, E. Salehpour, Digestion of restriction enzyme for the detection of single-base mismatch in DNA, Anal. Biochem. 421 (2012) 125–129.

[13] H. Wang, H. Li, Y. Huang, M. Xiong, F. Wang, C. Li, A label-free electrochemical biosensor for highly sensitive detection of gliotoxin based on DNA nanostructure/MXene nanocomplexes, Biosens. Bioelectron. 142 (2019), 111531.

[14] C. Li, X. Hu, J. Lu, X. Mao, Y. Xiang, Y. Shu, G. Li, Design of DNA nanostructure-based interfacial probes for the electrochemical detection of nucleic acids directly in whole blood, Chem. Sci. 9 (2018) 979–984.

[15] J. Ma, L. Xue, M. Zhang, C. Li, Y. Xiang, P. Liu, G. Li, An electrochemical sensor for Oct4 detection in human tissue based on target-induced steric hindrance effect on a tetrahedral DNA nanostructure, Biosens. Bioelectron. 127 (2019) 194–199.

[16] L. Liang, J. Li, Q. Li, Q. Huang, J. Shi, H. Yan, C. Fan, Single-particle tracking and modulation of cell entry pathways of a tetrahedral DNA nanostructure in live cells, Angew. Chem. 53 (2014) 7745–7750.

[17] K. Xia, H. Kong, Y. Cui, N. Ren, Q. Li, J. Ma, R. Cui, Y. Zhang, J. Shi, Q. Li, M. Lv, Y. Sun, L. Wang, J. Li, Y. Zhu, Systematic study in mammalian cells showing no adverse response to tetrahedral DNA nanostructure, ACS Appl. Mater. Interfaces 10 (2018) 15442–15448.

[18] Z. Fu, T. Lv, L. Jiang, C. Xing, C. Lu, Ultrasensitive electrochemical detection of microRNA based on in-situ catalytic hairpin assembly actuated DNA tetrahedral interfacial probes, Talanta 233 (2021), 122600.

[19] M. He, M. He, J. Zhang, C. Liu, Q. Pan, J. Yi, T. Chen, A spatial-confinement hairpin cascade reaction-based DNA tetrahedral amplifier for mRNA imaging in live cells, Talanta 207 (2020), 120287.

[20] I. Kim, D. Lee, S.W. Lee, J.H. Lee, G. Lee, D.S. Yoon, Coagulation-inspired direct fibrinogen assay using plasmonic nanoparticles functionalized with red blood cell membranes, ACS Nano 15 (2021) 6386–6394.

[21] E. Lanzi, S. Dinarelli, G. Longo, M. Girasole, V. Mussi, Multivariate analysis of mean Raman spectra of erythrocytes for a fast analysis of the biochemical signature of ageing, Talanta 221 (2021), 121442.

[22] R. Zhu, T. Avsievich, A. Popov, A. Bykov, I. Meglinski, In vivo nano-biosensing element of red blood cell-mediated delivery, Biosens. Bioelectron. 175 (2021), 112845.

[23] P. Wijesekara, Y. Liu, W. Wang, E.K. Johnston, M.L.G. Sullivan, R.E. Taylor, X. Ren, Accessing and assessing the cell-surface glycocalyx using DNA origami, Nano Lett. 21 (2021) 4765–4773.

[24] H.C.M. Yau, H.L. Chan, M. Yang, Electrochemical properties of DNA-intercalating doxorubicin and methylene blue on n-hexadecyl mercaptan-doped 5'-thiol-labeled DNA-modified gold electrodes, Biosens. Bioelectron. 18 (2003) 873–879.

[25] T. Zhang, Y. Gao, D. Xiao, J. Zhu, M. Zhou, S. Li, M. Zhang, Y. Lin, X. Cai, Nucleic acid based tetrahedral framework DNA nanostructures for fibrotic diseases therapy, Appl. Mater. Today 20 (2020), 100725.

[26] X. Chen, F. Tian, M. Li, H. Xu, M. Cai, Q. Li, X. Zuo, H. Wang, X. Shi, C. Fan, H. Baigude, Y. Shan, Size-independent transmembrane transporting of single tetrahedral DNA nanostructures, Glob. Chall. 4 (2020), 1900075.

[27] S. Dong, R. Zhao, J. Zhu, X. Lu, Y. Li, S. Qiu, L. Jia, X. Jiao, S. Song, C. Fan, R. Hao, H. Song, Electrochemical DNA biosensor based on a tetrahedral nanostructure probe for the detection of avian influenza A (H7N9) virus, ACS Appl. Mater. Interfaces 7 (2015) 8834–8842.

[28] W. Qin, L. Chen, Z. Wang, Q. Li, C. Fan, M. Wu, Y. Zhang, Bioinspired DNA nanointerface with anisotropic aptamers for accurate capture of circulating tumor cells, Adv. Sci. 7 (2020), 2000647.

[29] B.A. Linkletter, I.E. Szabo, T.C. Bruice, Solid-phase synthesis of deoxynucleic guanidine (DNG) oligomers and melting point and circular dichroism analysis of binding fidelity of octameric thymidyl oligomers with DNA oligomers, J. Am. Chem. Soc. 121 (1999) 3888–3896.

[30] S. Ramakrishnan, M. Palaniandavar, Mixed-ligand copper(II) complexes of dipicolylamine and 1,10-phenanthrolines: the role of diimines in the interaction of the complexes with DNA, J. Chem. Sci. 117 (2005) 179–186.

[31] C.A. Mitsopoulou, C.E. Dagas, C. Makedonas, Characterization and DNA interaction of the Pt(II)(pq)(bdt) complex: a theoretical and experimental research, Inorg. Chim. Acta. 361 (2008) 1973–1982.

[32] J. Lin, R. Liu, C. Gao, Interactions of L-Arg with calf thymus DNA using neutral red dye as a fluorescence probe, Spectrochim. Acta Mol. Biomol. Spectrosc. 97 (2012) 532–535.

[33] S. Kashanian, M.M. Khodaei, P. Pakravan, Spectroscopic studies on the interaction of isatin with calf thymus DNA, DNA Cell Biol. 29 (2010) 639–646.

[34] Y. Sun, X. He, J. Ji, M. Jia, Z. Wang, X. Sun, A highly selective and sensitive electrochemical CS-MWCNTs/Au-NPs composite DNA biosensor for Staphylococcus aureus gene sequence detection, Talanta 141 (2015) 300–306.

[35] C. Lin, Y. Wu, F. Luo, D. Chen, X. Chen, A label-free electrochemical DNA sensor using methylene blue as redox indicator based on an exonuclease III-aided target recycling strategy, Biosens. Bioelectron. 59 (2014) 365–369.

[36] F. Janku, J.J. Lee, A.M. Tsimberidou, D.S. Hong, A. Naing, G.S. Falchook, S. Fu, R. Luthra, I. Garrido-Laguna, R. Kurzrock, PIK3CA mutations frequently coexist with RAS and BRAF mutations in patients with advanced cancers, PLoS One 6 (2011), e22769.